

Photoionization Scheme for
Enrichment of Lu-176 1

Rejuvenating drying
springs in Himalayas 6

Advanced Mirror Alignment
System for Indus-2 16



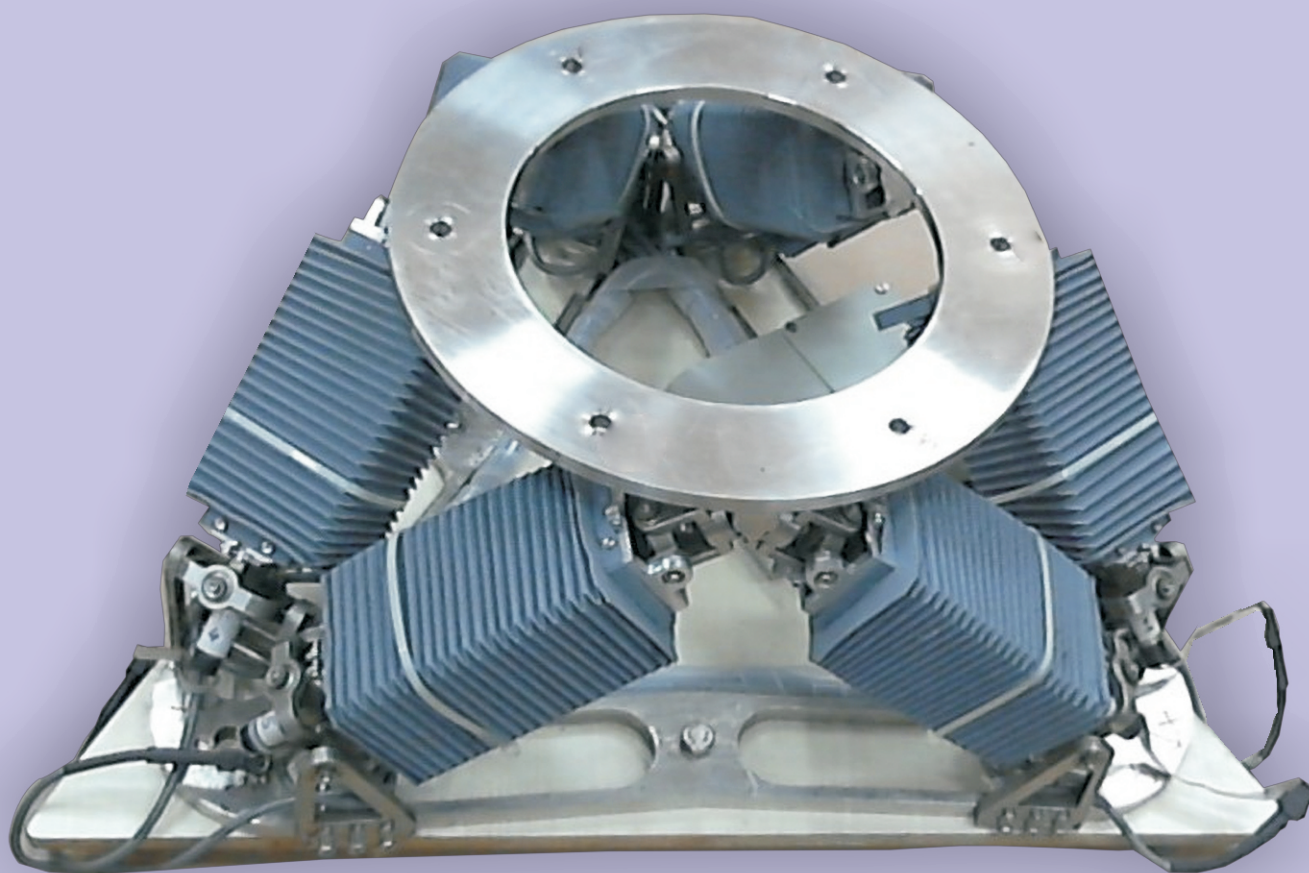
Bi-monthly • March - April • 2020

• Issue No. 373

ISSN: 0976-2108

BARC

NEWSLETTER



Parallel Mechanism Hexapod System for Indus-2

This page is intentionally left blank

CONTENTS

Editorial Committee

Chairman

Dr. A.P. Tiwari
KMG

Editor

Dr. G. Ravi Kumar
SIRD

Members

Dr. A.K. Nayak, RED
Dr. G. Sugilal, PSDD
Dr. V.H. Patankar, ED
Dr. (Smt.) B.K. Sapra, RP&AD
Dr. L.M. Pant, NPD
Dr. Ranjan Mittal, SSPD
Dr. (Smt.) S. Mukhopadhyay, ChED
Dr. K.P. Muthe, TPD
Dr. V. Sudarsan, ChD
Dr. A.V.S.S.N. Rao, MBD
Dr. S.R. Shimjith, RCnD
Dr. Sandip Basu, RMC
Dr. Pranesh Sengupta, MSD
Dr. R. Tripathi, RCD

Member Secretary

Shri Madhav N, SIRD

Issue Designed by

Shri Dinesh J. Vaidya, SIRD

Cover Page Photo Editing by

Shri Sunil Angrakh, SIRD

1

Novel Highly Selective Photoionization Scheme for Enrichment of Lu-176

Asawari D. Rath and S. Kundu

6

Rejuvenating drying springs in Himalayas

Tirumalesh Keesari, Uday Kumar Sinha, Hemant Mohokar, Harish Jagat Pant, Vinod Khatti and Pradeep Kumar Pujari

16

Advanced Mirror Alignment System for Indus-2 DEXAFS Beamline

Sumit Kumar Sinha, Abhishek Jaju, T. A. Dwarakanath, Gaurav Bhutani, K. Madhusoodanan, Debducta Lahiri, Nandini Garg, S. N. Jha and Ashutosh Dwivedi

This page is intentionally left blank

Novel Highly Selective Photoionization Scheme for Enrichment of Lu-176

Asawari D. Rath*, S. Kundu

Advanced Tunable Laser Applications Facility,
Beam Technology Development Group

Abstract

There is continually increasing demand of the radioisotope Lu-177 in radiopharmaceutical industry for diagnostic as well as therapeutic applications. Although not naturally abundant, it can be produced in nuclear reactor by neutron irradiation of its precursor isotope Lu-176. For high product yield, better than 80 % enriched Lu-176 is essential. We have constructed a novel photoionization scheme showing high spectroscopic selectivity and compatible with the existing process laser facility for selective photoionization of Lu-176 from its natural composition.

Keywords: Enrichment of Lu-176, selective resonant photoionization scheme, TOFMS

Introduction

The radio-isotope Lutetium-177 finds extensive applications in medical sector for diagnostics and treatment of certain types of cancers. At present, the use of Lu-177 is in radiopharmaceutical industry and its demand is continually increasing in India and there is a growing need of indigenous technology development for production of Lu-177 of required purity. It is not abundant naturally, nevertheless can be produced in nuclear reactors; one of the production routes being neutron irradiation of its precursor Lu-176. In order to obtain Lu-177 with high specific activity and required isotopic purity, the lutetium sample to be irradiated is required to be enriched in Lu-176 from its natural abundance of 2.6% to typically better than ~80%¹.

Laser based selective photo ionization (PI) and subsequent collection of the desired isotope is a very lucrative separation technology, particularly for medical isotopes where typical product requirement is in the range of few milligram to gram. This

technology relies on employing a multi-step PI ladder for selective excitation and subsequent ionization of the desired isotope with each transition step chosen in order to facilitate optimum isotopic selectivity as well as efficient ion yield of the selected isotope. Currently there are many groups working towards realization of commercial scale enrichment of Lu-176 using laser based atomic isotope separation^{2,3}. These groups employ either two-step or three-step resonant photoionization schemes for selective photoionization of Lu-176.

In Beam Technology Development Group, existing laser facility comprises of high repetition rate tunable dye lasers that are pumped by copper vapour lasers (CVL) and diode pumped solid state lasers (DPSSL) and are capable of delivering high powers over prolonged hours of operation in the wavelength range 550-610 nm with the use of Rhodamine group dyes in aqueous solvents. Keeping in view this already

available laser infrastructure, it is prudent to construct a three-step PI scheme for isotope separation of Lu-176 by atomic route which is compatible with the existing infrastructure with constituent wavelengths in suitable range.

Lutetium Atomic Structure

The three valence electrons in lutetium give rise to relatively simpler atomic structure with sparsely distributed energy levels leading to fewer atomic lines. It has two naturally occurring isotopes : Lu-175 (97.41%) and Lu-176 (2.59%); both exhibit hyperfine structures. The isotope shifts of Lu spectral lines are typically in sub-GHz range while typical hyperfine spreads of the transitions may be up to few GHz. Consequently the isotope selectivity invoked by a PI scheme roots from the separation between hyperfine components of Lu-175 and Lu-176 for constituent step transitions rather than their isotope shifts. This necessitates selection of transitions with broad spread in their hyperfine envelope.

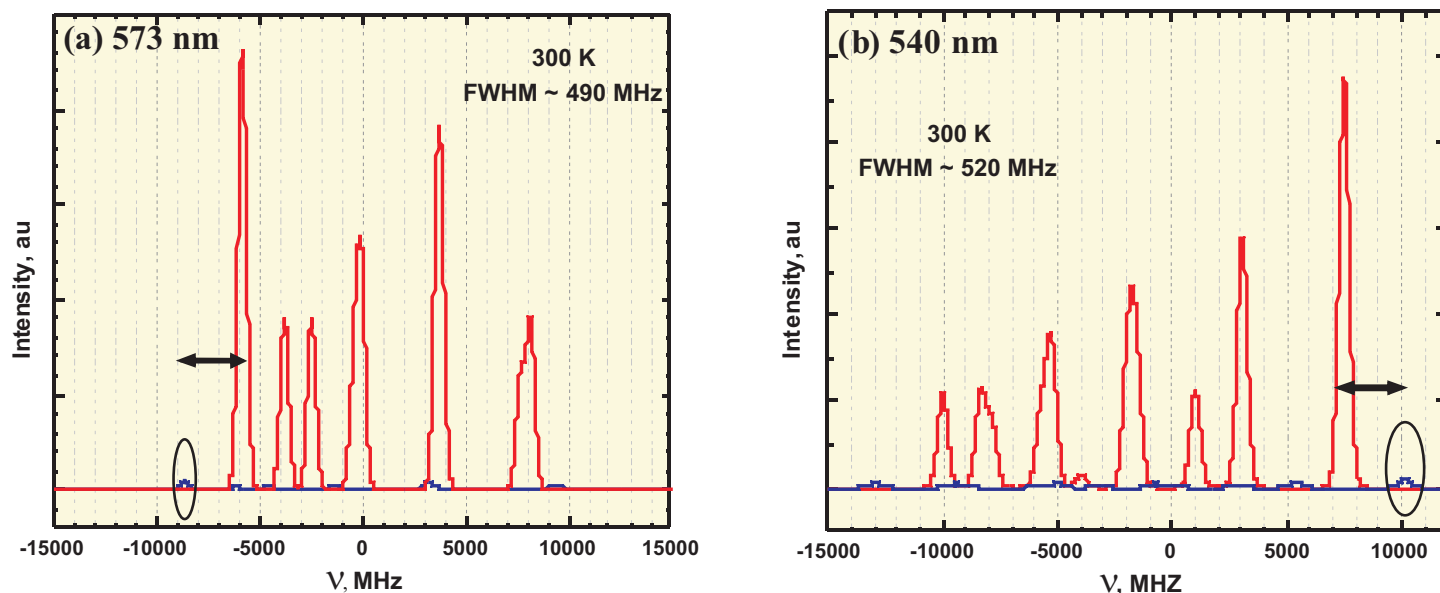


Fig.1: Simulated hyperfine spectra of natural Lu isotopes Lu-175 (red) and Lu-176 (blue) at Doppler temperature of 300 K for the transitions at (a) 573 nm and (b) 540 nm. The isotopes are in their natural abundance. The centre of gravity of HFS of Lu-175 lies at $v=0$. The hyperfine component of Lu-176 targeted for selective ionization is marked by ellipse.

First step transition

Lu atomic structure offers only two suitable transitions at 540 nm and 573 nm for first step excitation from ground level that fall in the domain of available process lasers⁴. Both the transitions are well-characterized in literature for their hyperfine profiles and isotope shifts⁵. Simulated hyperfine envelopes of these transitions for both Lu isotopes⁴ Lu-175 and Lu-176 corresponding to Doppler temperature of 300 K are shown in Fig.1 (a) and (b). For both the transitions, there is clear separation (shown by arrow) of 2.6 GHz between the strongest hyperfine component $F=17/2$ $F'=17/2$ of Lu-176 targeted for selective excitation (marked by ellipse) and nearest hyperfine component of Lu-175. As a consequence, the first step isotopic selectivity provided by either of them is of similar extent. Enrichment of Lu-176 has been demonstrated² using PI scheme based on 540 nm as first step. However, this three-step PI scheme comprised of

540 nm-535 nm-618 nm transitions is not very convenient for generation of high power dye laser output at constituent transitions as may be required by the process. Further, the isotope selectivity offered by this scheme is mainly contributed by the first step transition.

Consequently, we decided to explore 573 nm as the first step in PI ladder, which excites the Lu atoms in ground level to the level at 17427.28 cm^{-1} . This article presents the outcome of RIMS experiments performed using a two-step and a three-step resonant photoionization of Lu in an indigenously developed time of flight mass spectrometer (TOFMS) towards construction of an isotope selective PI scheme using 573 nm as first excitation step. Further, we have demonstrated experimentally 84% enrichment of Lu-176 in TOFMS.

RIMS Set-up

Schematic of the experimental set up for multi-step multi-colour resonance ionization mass spectroscopy is

shown in Fig 2. Three dye lasers DL-1 to DL-3 pumped by second harmonic of an Nd:YAG laser provide first, second and third step excitation photons respectively. Optical delays of 10 ns and 2-3 ns, respectively, were introduced between the pulses from (DL-1, DL-2) and (DL-2, DL-3), to ensure sequential arrival of the pulses at the laser-atom interaction zone of an indigenously developed TOFMS. An atomic beam generator integrated with the TOFMS delivered well collimated beam of Lu atoms in the interaction region to spatially overlap with all the three dye laser beams. The photoions generated were directed by use of DC electric fields to an MCP detector through the mass analyser module of TOFMS with resolution ~ 200 amu. Mass spectra thus obtained were recorded simultaneously using a digital storage oscilloscope and two gated integrators adjusted to detect mass peaks of Lu-175 and Lu-176 respectively. Parts of the lasers were sent to a wavelength meter for monitoring and recording laser

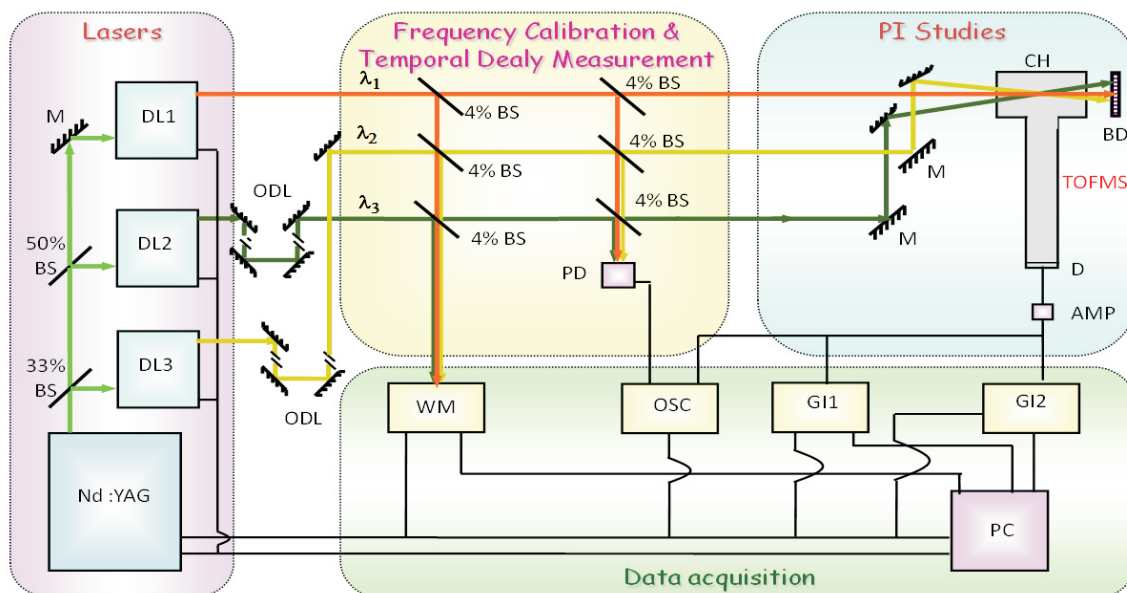


Fig.2: Schematic of the experimental set-up for multi-step multi-colour resonance ionization mass spectroscopy (RIMS). The abbreviations used are as follows: Nd:YAG: Nd:YAG laser; DL1-3: dye lasers; M: mirror; BS: beam splitter; ODL: optical delay line; CH: photoionization chamber; TOFMS: time of flight mass spectrometer; BD: beam dump; D: micro channel plate detector; AMP: amplifier; WM: wavelength meter; PD: photodiode; GI1-2: gated integrators; OSC: oscilloscope; PC: personal computer for data acquisition and control of lasers. In two-colour RIMS DL-3 output is blocked.

wavelengths while their tuning/scanning. A data acquisition system was used to control scanning of lasers and record the outputs of gated integrators and wavelength meter concurrently.

Second step transition

There is no excitation pathway available in literature from the energy level at 17427.28 cm^{-1} . From the available databases⁶ of Lu I energy levels, possible transitions from this level allowed by selection rules were shortlisted as 560 nm, 609 nm and 642 nm. Among these, a transition $17427.28 \text{ cm}^{-1} \rightarrow 33831.46 \text{ cm}^{-1}$ at 609 nm was confirmed in two-photon resonant RIMS experiments, in which DL1 was tuned to centre of gravity of 573 nm transition of Lu-175 and DL2 was scanned across 609 nm. Further, it showed significant signal strength as well as very broad HFS width, which is highly desirable to achieve high second step selectivity of the PI ladder. This transition was used as second step excitation in subsequent three-step

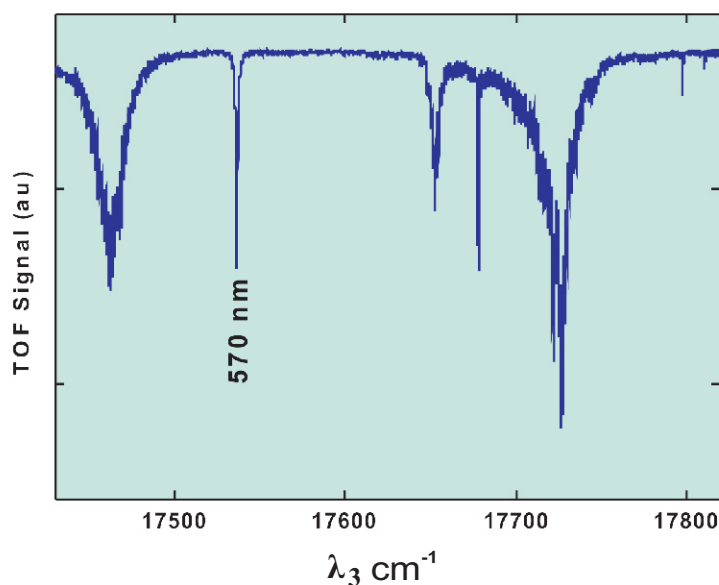


Fig.3: Three-photon resonant RIMS spectra of Lu-175 in TOFMS showing autoionization resonances originating from the Lu I level at 33831.46 cm^{-1} . Here λ_1 and λ_2 were tuned to centres of gravity of 573 nm and 609 nm transitions respectively. The narrow autoionization resonance at 570 nm with clean background was selected as ionizing transition for selectivity experiments on Lu-176.

photoionization experiments to explore suitable third step exciting the atoms to odd parity autoionization levels of Lu I followed by ionization.

Third step transition

To explore suitable autoionization resonances for third step of the

selective PI scheme, three-photon resonant RIMS experiments were performed on Lu-175 with DL-1 and DL-2 tuned to centres of gravity of 573 nm and 609 nm transitions respectively and DL-3 was scanned. The resulting photoionization spectra are presented in Fig.3. For high overall

selectivity of a PI scheme, the autoionization resonance needs to have narrow line width and high signal strength. A strong and narrow resonance at 570 nm fulfilling these requirements was selected as third step to complete the selective photoionization ladder shown in Fig.4.

Demonstration of selective ionization of Lu-176

The experiments to construct the novel photoionization scheme shown in Fig.4 were performed on Lu-175 owing to its high natural abundance. However, for selectivity demonstration of Lu-176, the lasers are required to be tuned to Lu-176 spectral lines. Consequently, DL-1 was tuned to the $F=17/2 \rightarrow F'=17/2$ hyperfine component of 573 nm transition of Lu-176 so as to selectively populate this upper hyperfine sub-level of first excitation level of Lu-176. Exact wavelength of this component was derived from the isotope shift IS (Lu-175, Lu-176) and hyperfine structure simulations and verified experimentally. Further, DL-2 was scanned through 609 nm to locate the $F'=17/2 \rightarrow F''=17/2$ hyperfine component of Lu-176 for this line and DL-2 was subsequently tuned to this component. The ionizing laser DL-3 was then tuned to maximize the Lu-176 ion signal. The selectivity has a strong dependence on laser intensities as at higher intensities saturation broadening enhances ionization of undesired isotope Lu-175 thereby reducing overall enrichment. The laser intensities were optimized in order to minimize this effect. At laser pulse energies of 5 μJ (573 nm), 25 μJ (609 nm) and 200 μJ (570 nm) corresponding to beam

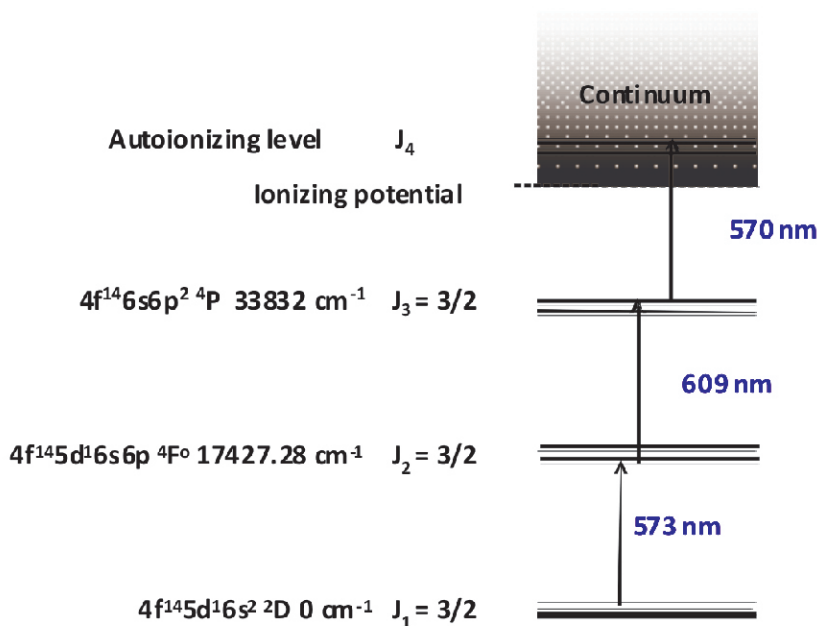


Fig.4: Schematic of the highly selective novel PI scheme for enrichment of Lu-176.

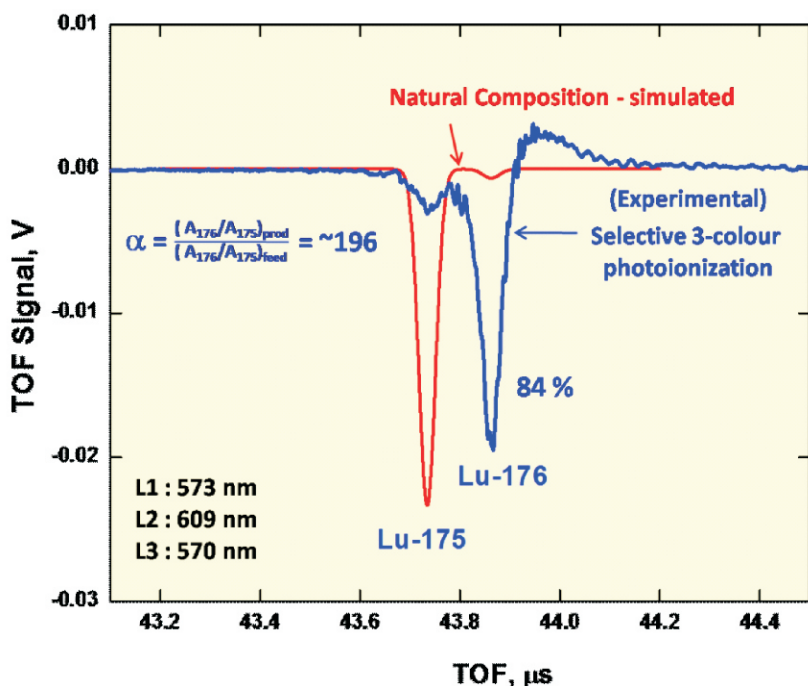


Fig.5: Selective ionization of Lu-176 from natural sample using novel photoionization scheme. The lasers are tuned to selected Lu-176 hyperfine transitions as described in text. The red graph (simulated) shows natural abundance while blue graph shows mass spectrum recorded experimentally using the novel PI scheme. Analysis of spectrum indicates enrichment of Lu-176 to 84% from its natural abundance A_{176} of 2.59% with enrichment factor of ~196.

cross-sectional area of $\sim 7 \text{ mm}^2$, an enrichment of $> 80\%$ was realized for Lu-176 despite use was made of multi-mode lasers with $\sim 2 \text{ GHz}$ typical line widths. Fig.5 shows

experimentally recorded mass spectrum (in blue colour) showing 84% enrichment of Lu-176. With the advent of single mode lasers recently developed in house with typical line

widths 100 MHz, the selectivity is expected to enhance further and will enable use of higher intensities essential for efficient ionization of Lu-176, thus, enhancing both quality and quantity of the enriched product.

Conclusion and Future Scope

The novel three-step photoionization scheme with 573 nm - 609 nm - 570 nm transitions is superior to the reported scheme 540 nm – 535 nm – 618 nm for Lu-176 isotope separation in terms of overall selectivity. Further, it is compatible with existing capabilities of process laser infra-structure in terms of generating requisite high laser powers at high repetition rates, single mode operation, etc. Development of a prototype separator and process lasers pertaining to this novel scheme is in progress. The high spectroscopic selectivity offered by this scheme combined with the use of single mode process lasers has potential for significant enhancement in both enrichment factor and process throughput in the production of enriched Lu-176 from natural composition.

***Corresponding author**

Dr. Asawari D Rath

Acknowledgements

Authors thank Dr. Archana Sharma, Associate Director, BTDG, for her interest and constant support during this work. Thanks are due to R.K. Rajawat, former Associate Director, BTDG for his interest and support during initial stages of the work.

References

1. Radiochemistry and Isotope Group, BARC.
2. D'yachkov A.B., Firsov V.A., Gorkunov A.A., Labozin A.V., Mironov S.M., Panchenko V.Y., Semenov A.N., Shatalova G.G., Tsvetkov G.O., "Selective photoionisation of lutetium isotopes", Quant. Electron. 42, 953-956 (2012).
3. Gadelshin V., Cocolios T., Fedoseev V., Heinke R., Kieck T., Marsh B., Naubereit P., Rothe S., Stora T., Studer D., Van Duppen P.,

Wendt K., "Laser resonance ionization spectroscopy on lutetium for the MEDICIS project", Hyperfine Interact., 238: 28 (2017).

4. Rath Asawari D., "Lutetium Isotope Separation by AVLIS route : Assessment of Spectroscopy and Selectivity Physics Towards Enrichment of Lu-176", BARC Internal report BARC/2019/I/024 (2019).
5. Kuhnert A., Nunnemann A. and Zimmermann D., J. Phys. 16B, 4299 (1983).
6. Ralchenko Yu., Kramida A.E., Reader J., NIST Atomic Spectra Database, <https://www.nist.gov/pml/atomic-spectra-database>; Kurucz R.L., Bell B., Atomic Line Data, Smithsonian Astrophysical Observatory, Cambridge, Kurucz, CD-ROM# 23, 1995.

Applications of Isotope Technology

Rejuvenating drying springs in Himalayas

Tirumalesh Keesari*, Uday Kumar Sinha, Hemant Mohokar, Harish Jagat Pant

Isotope and Radiation Application Division, Bhabha Atomic Research Centre, Mumbai-400 085

Vinod Khatti

Himalayan Environmental Studies and Conservation Organization (HESCO), Dehradun,
Uttarakhand

Pradeep Kumar Pujari

Radiochemistry and Isotope Group, Bhabha Atomic Research Centre, Mumbai-400 085

Abstract

Reduction in spring discharge is being experienced as a common phenomenon across the Himalayan region due to the impact of climate change on precipitation patterns and rainfall intensity, reduction in its frequency and a marked decline in the winter rainfall. There is a wide gap in knowledge about the Himalayan springs due to inadequate investigations, inaccessibility, lack of well-proven methodologies for studying the mountainous springs and over and above, lack of compilation of existing information in published literature. Naturally occurring and anthropogenic/manmade isotope techniques have proved to be effective tools providing vital information that could not be obtained by any other means and helped to solve critical hydrological problems. This article describes the potential of isotope techniques in identifying the recharge zones of drying springs in the Himalayan region. The studied springs belong to two sites in Uttarakhand, viz., Pipaya (Dehradun dist.) and Brahmkhal (Uttarkashi dist.). The isotopes used in this study are naturally occurring isotopes of constituent elements of water molecule, viz., stable (^2H & ^{18}O) and radioactive (^3H). Stable isotope variations provide the dominant recharge altitude for the spring recharge while radioisotope data provide information on the residence time of the spring water. The isotope findings are integrated with the local geological, hydrogeological and geomorphological information to plan the construction of appropriate rainwater harvesting structures at identified recharge altitudes. This study has resulted in formulating policies on a national scale for reviving the drying springs through isotope technology.

Keywords: ^2H , ^{18}O , ^3H , Isotope tracers, Drying springs, Himalayas, Pipaya, Brahmkhal, Gabion check dams

Introduction

Himalayan ranges stretch 2500 km along the northern border of India and are host to numerous natural springs. Nearly 50 million people reside in the Indian Himalayan Region (http://gbpihedenvi.nic.in/him_state.s.htm). The mountain communities are highly dependent on spring water for both domestic and irrigation purposes. On an average there are two to three springs in each village with discharges varying between 3 and 4

liter/min. Natural stressors (especially climate change) and improper watershed management have led to a steady decline in discharge rates of many Himalayan springs (Agarwal et al., 2012). Valdiya and Bartarya (1989) reported a 40% reduction in spring discharge over a 35-year period (1951 to 1986) in the Kumaun Himalaya region, which was mostly attributed to changes in land-use patterns and vegetation. In another study, Mahamuni and Kulkarni (2012) identified that nearly 8,000 villages

are facing acute water shortages due to the drying up of springs in the Himalayan region. The Niti Aayog reported that high surface run off due to changing land use pattern along with increased water demand, ecological degradation and climate change are the major factors impacting the spring discharges and drying up of springs (Gupta and Kulkarni, 2018). Similar concerns of drying up of perennial springs in the Himalayan region of India have led to many initiatives by a various

non-profitable organization to revive and conserve these springs (Pant and Rawat, 2015).

Intensive spring studies have been taken up predominantly in the western Himalayan region focussing on aspects pertaining to spring discharge in relation to rainfall patterns and catchment degradation (Bartarya, 1991; Bonacci, 1993). These studies showed that the spring discharge is a function of both the rainfall pattern as well as the recharge area characteristics such as the slope of the ground surface, surface cover, geology of the area and permeability of topsoil. Watershed interventions can aid in augmenting spring discharge. However, site-specific data are needed to implement successful watershed interventions. Vashisht (2008) indicated that, if springs and small seepage canals are managed properly in the Siwalik foothill regions of the Himalayas, water scarcity could be averted. Numerous watershed interventions have been attempted in the past to improve water availability for rural communities in the Himalayan regions. However, most interventions were not site-specific and did not take in to account karst geology and preferential pathways in aquifers (Agarwal et al. 2012). Furthermore, studies to assess the impact and sustainability of these interventions are rare, especially to quantify their impact on spring discharge. Bruijnzeel and Bremmer (1989) and Alford (1992) concluded that the current understanding of hydrological processes in the Himalayas is inadequate, and management plans stemming from inadequate understanding would not solve water scarcity challenges.

Therefore, drying up of springs and water scarcity issues underscore the need to increase the understanding of spring hydrology, especially in the Himalayan region.

Environmental and artificial radioactive isotopes have proved to be effective tools for solving many critical hydrological problems and in several cases provided information that could not be obtained by any other methods (Clark and Fritz, 1997; Kendall and McDonnell, 1998; Rao, 1984). Environmental isotopes (stable and radioactive) have a distinct advantage over artificial tracers as they facilitate the study of various hydrological processes on a much larger temporal and spatial scales through their natural variation in a system, while the use of artificial tracers is generally confined to site-specific and local applications

(Keesari et. al., 2007; Rangarajan and Athavale, 2000; Kulkarni, 1992). Environmental isotopic techniques in conjunction with conventional hydrogeological and geochemical information can be employed to understand the recharge source/s of spring and to locate its recharge area/s for taking effective measures for its sustainability. Very few researchers have used isotopes to identify recharge areas in the Himalayas. Shivanna et al. (2008) have applied isotope techniques to identify the recharge altitudes of drying springs in Gaucher area of Rudraprayag District, Uttarakhand. The study identified the effect of altitude on spring behavior and guided the introduction of artificial rainwater harvesting recharge structures at specified sites identified by isotope technology. This increased the spring

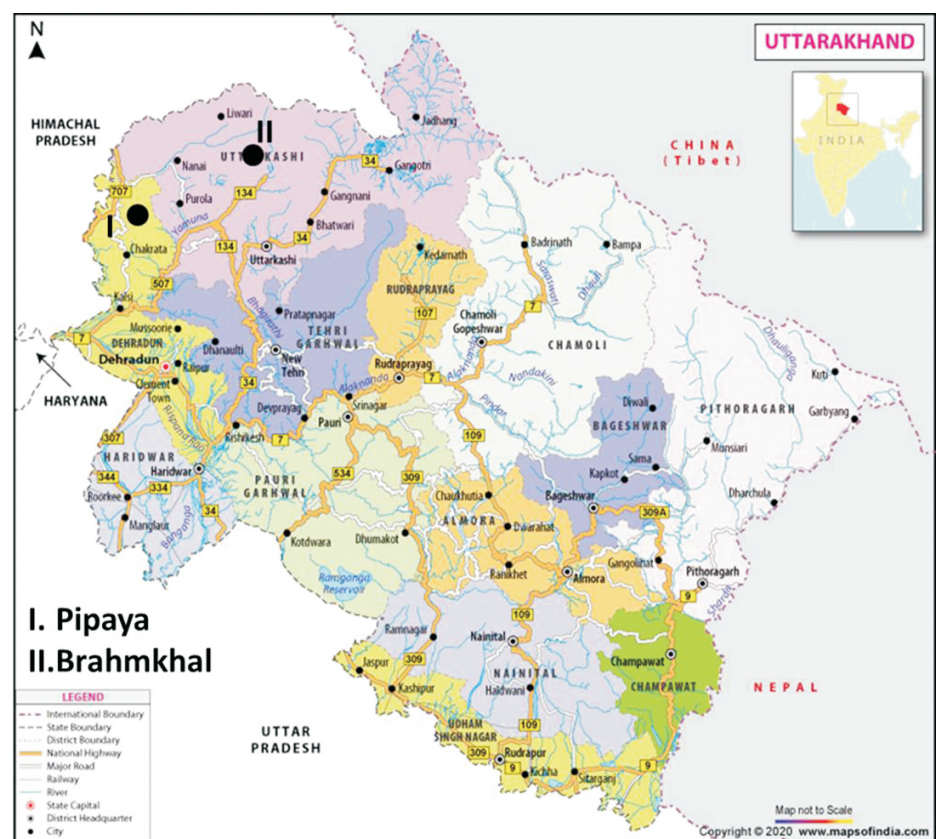


Fig.1: Location map of investigated sites in Uttarakhand (I. Pipaya and II. Brahmakhal)

discharges by 3 to 5 times and most importantly the springs were not dried up during summer months. Jeelani et al. (2010) used environmental isotopes to study the spring hydrology in Lidar watershed, Western Himalaya. The study concluded that the springs were mostly fed by rainfall. The springs and streams followed similar isotope trends, indicating that they were hydrologically connected. These studies demonstrated that isotope techniques could assist in identifying the spring sources and the transit times, thereby improving the overall understanding of spring hydrology.

In Uttarakhand state, the potable water for domestic use is largely derived from shallow wells (Naula) and springs (Dhara). Currently 30% of the springs have dried up and an additional 45% of the springs are on the verge of drying up (Agarwal et al., 2012; Mahamuni and Kulkarni, 2012; Tambeet. al., 2012). It is also estimated that 60% of the population is affected due to the drying up of the springs and over 10,000 villages have been classified as water-scarce villages (Pant and Rawat, 2015). In order to increase the spring discharges, it is essential to identify the dominant recharge zones of these drying springs and construct suitable artificial recharge structures for rainwater harvesting. This article highlights the role of environmental isotopes in reviving the drying in two sites viz., Pipaya (Dehradun dist.) and Brahmkhal (Uttarkashi dist.) in Uttarakhand state (Fig. 1).

Pipaya site is located about 80 km north to Dehradun the spring sites are shown on Google earth map (Fig. 2 I). There are ten springs distributed in

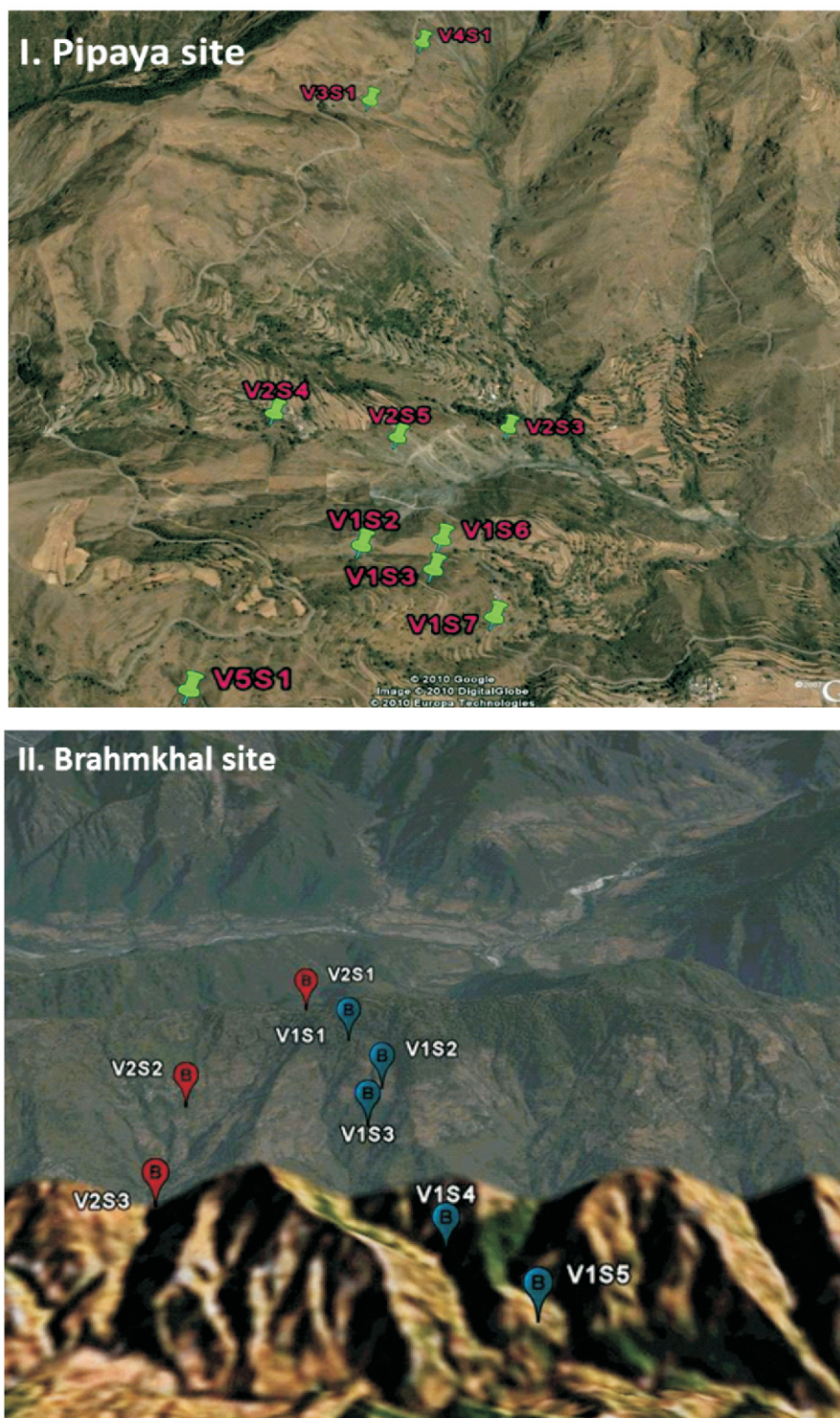


Fig.2:Google earth map of springs in I) Pipaya and II) Brahmkhal sites (V-Valley, S-Spring)

two main valleys and one spring in each of three sub valleys with elevations ranging from 1350 to 1650 m amsl. These springs cater to the water needs of almost 10,000 population. Brahmkhal site belongs to Uttarkashi district located about 40 km west of Uttarkashi city. There are

eight springs distributed in two valleys and the elevation of these springs ranges from 1200 to 1760 m amsl (Fig. 2 II). A total of 5000 population uses the spring water.

Isotope Techniques

Stable isotopic composition of water ($\delta^2\text{H}$ and $\delta^{18}\text{O}$) is modified by

evaporation and condensation. As water evaporates from the ocean surface, the lighter isotopes (^1H and ^{16}O) preferentially move to the vapour phase because of the difference in vapour pressures and diffusion velocities. The resulting vapour mass is depleted in heavier isotopes (^2H and ^{18}O) as compared to lighter isotopes (^1H and ^{16}O). A reverse trend is noticed when vapour condenses to liquid (or solid), i.e., heavier isotopes get concentrated in rain compared to the remaining vapour. The former process takes place under non-equilibrium condition (kinetic effect), whereas the latter process occurs under equilibrium condition (thermodynamic effect). This allows the recharge water in a particular environment to have a characteristic isotopic signature. This signature, though minute, serves as a natural tracer for water movement. The minor variations in the isotope signature are normally expressed as relative isotope concentrations with respect to a standard and can be determined with the desired accuracy by an isotope ratio mass spectrometer. The relative difference is denoted by “ δ ” and is computed as (Craig, 1961);

$$\delta = \left(\frac{R - R_{std}}{R_{std}} \right) \times 10^3 \text{‰}$$

where R represents the isotope ratio of a sample ($^2\text{H}/^1\text{H}$ and $^{18}\text{O}/^{16}\text{O}$) and R_{std} represents the corresponding ratio in the standard. The value is generally expressed in parts per thousand (per mil, ‰). $\delta^2\text{H}$ and $\delta^{18}\text{O}$ values are reported relative to Vienna Standard Mean Ocean Water (VSMOW).

Applications of stable isotope ratios of hydrogen and oxygen in water are

primarily based upon the isotopic variations in precipitation (Clark and Fritz, 1997; Kendall and Caldwell, 1998). Globally, $\delta^2\text{H}$ and $\delta^{18}\text{O}$ of precipitation show a good correlation given by; $\delta^2\text{H} = 8 * \delta^{18}\text{O} + 10$ and is known as Global Meteoric Water Line (GMWL). The isotopic composition of precipitation is affected by season, latitude, altitude, amount and distance from the coast. In addition, the variation in local climatic conditions and source of the moisture affect the isotopic composition of precipitation, and therefore the Local Meteoric Water Line (LMWL) needs to be constructed for each location under the study. In regions with altitude difference, orographic precipitation occurs as vapor mass rises over the landscape. The cooling of saturated air mass causes condensation and releases some heat counteracting the cooling. This temperature change with altitude is called ‘wet adiabatic lapse rate’, which varies with altitude and is about $0.6 \text{ }^\circ\text{C}$ per 100 m. Since the isotopic composition is temperature-dependent, the isotopic composition of precipitation depletes with altitude. The altitude effect generally varies from -0.15 to -0.5‰ for $\delta^{18}\text{O}$ and from -1 to -4‰ for $\delta^2\text{H}$ per 100 m. This altitude effect is used to identify the recharge altitudes in the mountainous regions (Shivanna et al., 2008; Jeelani et al., 2010 & 2015).

Environmental tritium (^3H) is produced due to the cosmogenic nuclear reactions and atmospheric nuclear testing that took place up to the early 1960s. After production, the ^3H atoms get oxidised and become a part of the hydrological cycle. Tritium concentrations are expressed in tritium unit (TU), where one TU

corresponds to one tritium atom per 10^{18} atoms of hydrogen, which is equivalent to a specific activity of 0.12 Becquerel (Bq) per litre of water. The hydrosphere is labeled on a local and global scale with ^3H , hence the measurement of ^3H concentration changes in time and space can provide information on the dynamics of water bodies. The most important use of tritium as a hydrologic tool is in the study of residence time of groundwater and surface manifestations of groundwaters such as small springs and seeps. At the simplest level, the presence of ^3H (normally above 1 TU) in springs implies that the water in the spring discharges has been recharged during the last 50 years.

Sampling and measurement

One important pre-requisite for a good investigation is the proper sampling followed by accurate measurements. Samples are collected from the fresh spring discharges (not stored water) from the two sites. For ^2H and ^{18}O sampling, the sample water is filled up to brim in a 25 ml capacity bottle while one litre of sample is collected for ^3H measurement. Samples are collected during pre-monsoon and post-monsoon period for two consecutive years (2009-2010). A total of 18 springs were sampled (Pipaya site – 10 and Brahmkhal site – 8) for isotope measurements. Rainwater samples for isotopes are also collected in a similar way from different altitudes spacing at least 100 m intervals from the investigation sites. Monthly discharge rates of all springs are also measured during the period of investigation.

Isotope ratio mass spectrometry (dual inlet GEO 20-20) is used for

measuring stable isotope ratios. In this, H₂ gas is equilibrated with the water sample in a closed bottle allowing isotopic exchange. The equilibrated hydrogen gas is measured for ²H/¹H ratio of the sample. Similarly, the ¹⁸O/¹⁶O ratio in water samples is measured by equilibrating carbon dioxide gas with the water sample at 50°C temperature and subsequently measuring the isotopic composition of the equilibrated CO₂ gas. The precision of measurement (2σ, 95% confidence level) was found to be 0.5‰ and 0.1‰ for δ²H and δ¹⁸O respectively. For tritium (³H) measurement, the sampled water is distilled and about 250 mL of the distillate is electrolytically enriched at a low temperature (1- 4 °C). The enriched sample is mixed with a scintillator mixture (8:12 mL) and counted in an ultra-low background (0.5 cpm) liquid scintillation counter (Quantulus model 1220). The minimum detection limit for this method is 0.5 TU (2σ) for 500 minutes counting. The counting efficiency and the calibration factor of the counter are about 25% and 70 TU/cpm respectively.

Results and discussion

a) Spring discharge trends

The discharge of the springs at Pipaya site ranges from 0.1 lit/min to 22 lit /min. In general, the low altitude springs of the respective valleys show higher discharges compared to high altitude springs. This indicates that the catchment area for the high altitude springs is less compared to low altitude springs. Even though the maximum discharge of each spring is quite different but the minimum discharge is of the same order

(Fig. 3a). The high discharges of the springs in 2008 and 2010 during Aug/Sep compared to the same period in 2009 is due to high rainfall during 2008 and 2010. The discharges of the springs are maximum in the month of September after the high precipitation in Jul/Aug. This indicates that all the springs are mainly recharged by

precipitation and the residence time of the recharged waters is short. Spring discharge data of Brahmekhal site shows that highest discharge 30 lit/min is found in V1S5 whereas lowest discharge is found in V1S3 which dried from Jul. 2009 to Jul. 2010. Three springs V1S1, V1S5 and V2S2 show high discharges (about 25-

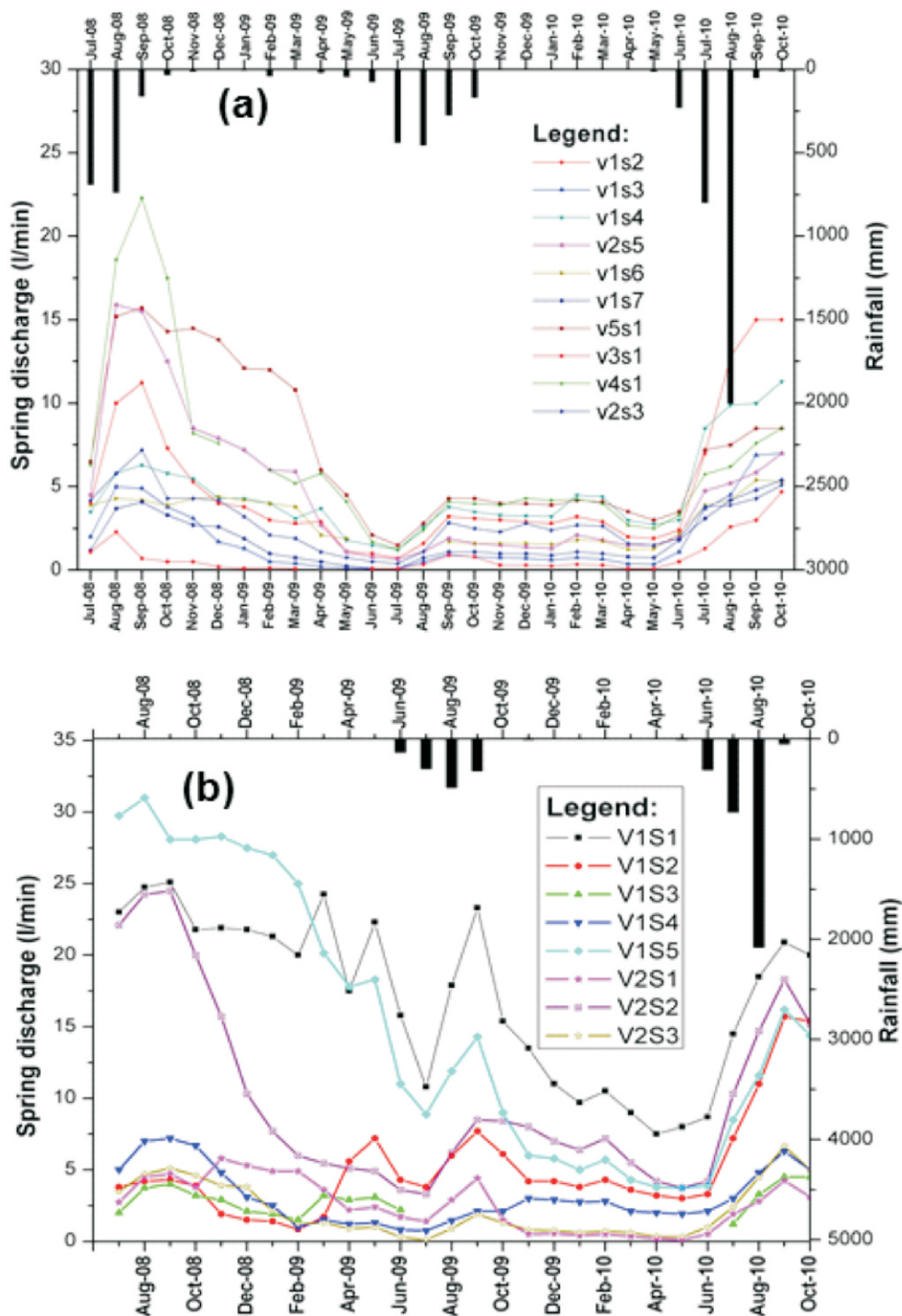


Fig.3: Spring discharges during 2008-2010 in a) Pipaya and b) Brahmakhal sites. Bars on the top axis represent rainfall amount. The spring Ids are as shown in Fig. 2. V – Valley and S - Spring

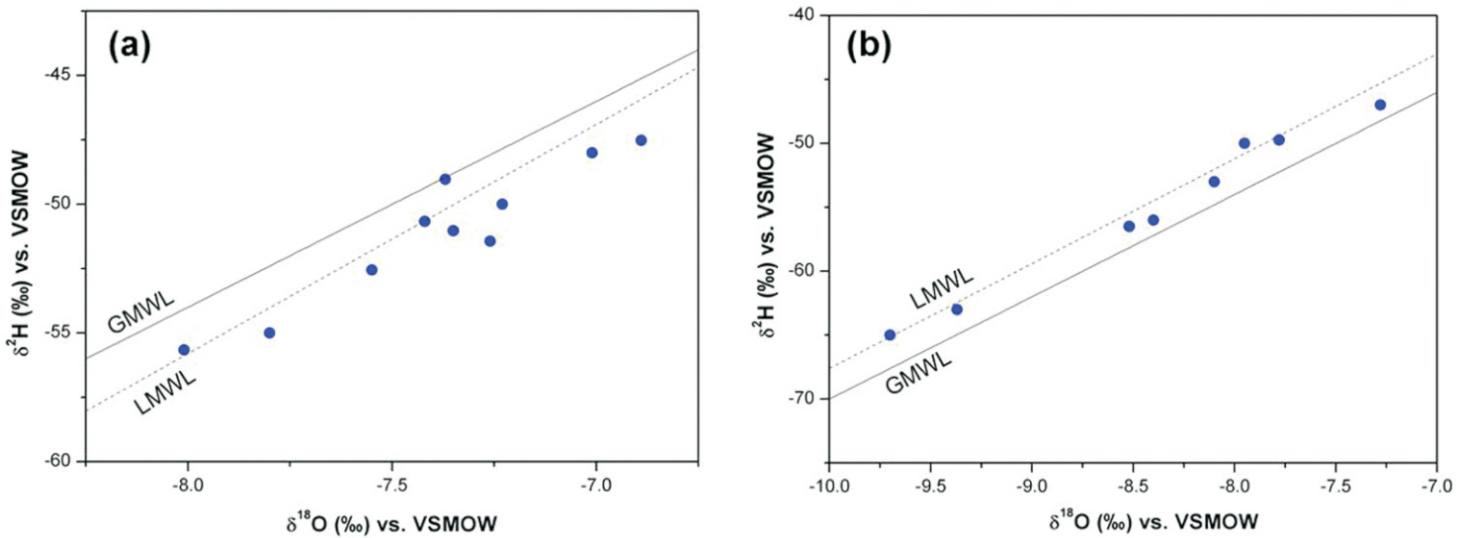


Fig.4: Plots of $\delta^2\text{H}$ versus $\delta^{18}\text{O}$ plot of spring samples of a) Pipaya and b) Brahmkhal sites

30 lit/min) and decrease to a minimum of 5 lit/min during dry period (Fig. 3b). These springs seem to be potential water sources and suitable artificial recharge measures can be planned at these spring sites.

b) Isotope signatures of spring waters

The $\delta^{18}\text{O}$ and $\delta^2\text{H}$ values of local rainwater were used to construct the LMWL. All spring samples fall along the LMWL ($\delta^2\text{H} = 8.9 \delta^{18}\text{O} + 15.4$) except some samples, which fall on

the GMWL. This indicates that the major component of spring recharge is local precipitation.

Samples falling below the LMWL suggest evaporation of the infiltrating rainwater (Fig. 4a). In order to obtain the original rainfall isotope composition, the sample data falling below the LMWL are extrapolated to intersect the LMWL. The intersecting point represents the isotopic composition of the precipitation that is recharging the spring. It is observed

that the isotope composition of spring waters collected during postmonsoon indicates depleted values compared to premonsoon season. Tritium content of spring waters at Pipaya site varies from 5.9 to 8.4 T.U and the rainwater show 7.5 to 9.5 T.U. This indicates that the spring waters are recharged by modern precipitation.

c) Identification of dominant recharge zones

The altitude effect is estimated from the variation of rainwater isotopic

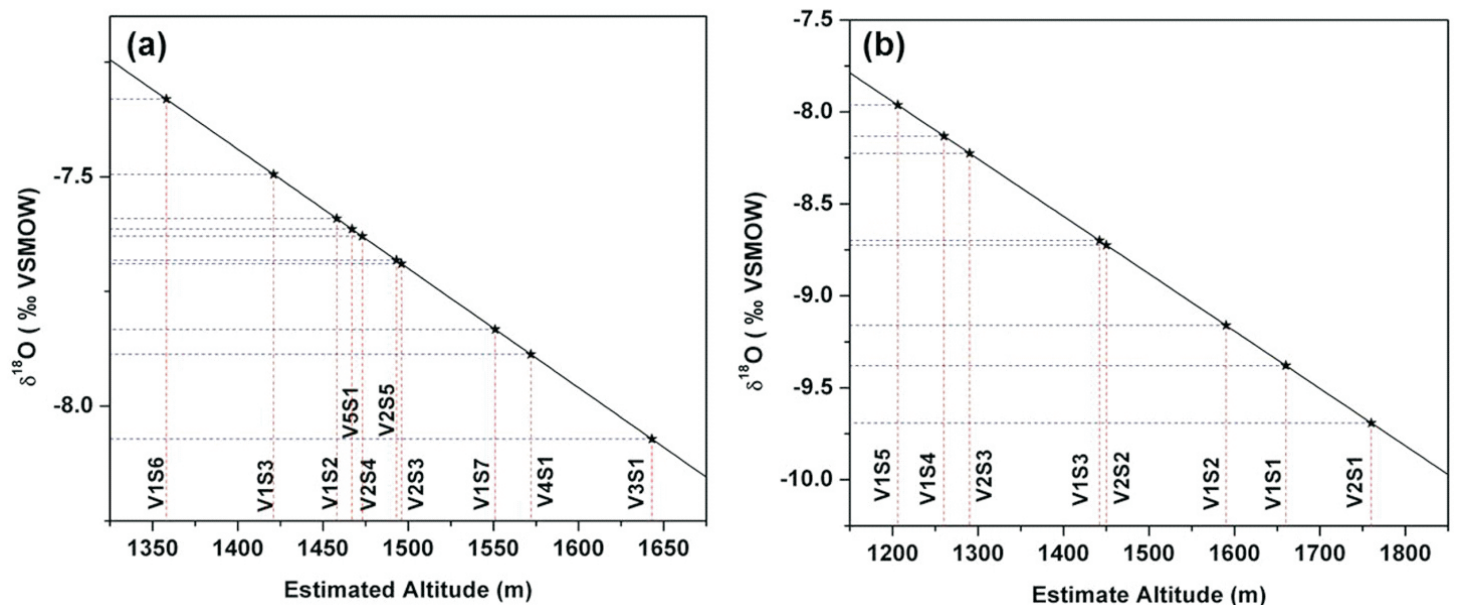


Fig.5: Plot of recharge altitude estimation based on altitude effect of precipitation in a) Pipaya and b) Brahmkhal sites. Line represents altitude effect in rainwater, V- Valley and S - Spring

composition with respect to altitude. An altitude effect at Pipaya site was found to be $-0.26\% \delta^{18}\text{O}$ per 100m rise in elevation. However, some samples did not show any specific altitude effect indicating possible contributions from multiple altitudes. In order to estimate the corresponding recharge altitude for the springs, the evaporation corrected value of the spring water is used in altitude effect equation (Fig. 5a). The line in the graph represents the best fit equation for the altitude effect obtained in that particular site. It is found that the dominant recharge altitudes are mostly between 1350m and 1500m above mean sea level (amsl). At Brahmakhal site, the altitude effect is calculated to be $-0.31\% \delta^{18}\text{O}$ per 100m. Altitude effects for both the sites fall within the range of naturally observed values (Clark and Fritz, 1997; Kendall and Caldwell, 1998). Based on the spring isotope value and

the altitude effect, the recharge altitude of the springs is estimated and found to range between 1200 and 1760m amsl, as shown in Fig. 5b. The lower altitude of recharge at to some springs could be due to contribution from irrigation return flow in this location.

Recharge to spring occurs when the rain water or surface water infiltrates downward through the soil to the water table and emerges as spring outlet. Artificial recharge (AR) is the process of spreading or impounding water on the land to increase the infiltration through the soil and percolation to the aquifer or of

injecting water by wells directly into the aquifer. AR is effective and economic if the recharge altitudes to the springs are known and due consideration is given to the geomorphological features of the area. Considering the geomorphological features at the identified recharge altitudes, suitable recharge structures are recommended for each site (Table 1). The recharge structures include; percolation tanks, infiltration pits, sub surface dykes, gabion check bund and contour trenches. The photographs of a few recharge structures constructed at the identified sites are shown in Fig. 6. In order to study the impact of

Table 1. Types of artificial recharge structures constructed

Site	Number of springs	District	Recommended structures
Pipaya	10	Dehradun	5 gabion check dams/bunds, 1 percolation pond and 3 staggered trenches
Brahmkhal	8	Uttarkashi	4 gabion check dams, 2 percolation ponds and 4 staggered trenches



Fig.6:various recharge structures constructed at the identified recharge zones, a) gabion check dam, b) infiltration pits, c) contour bunding and d) percolation ponds

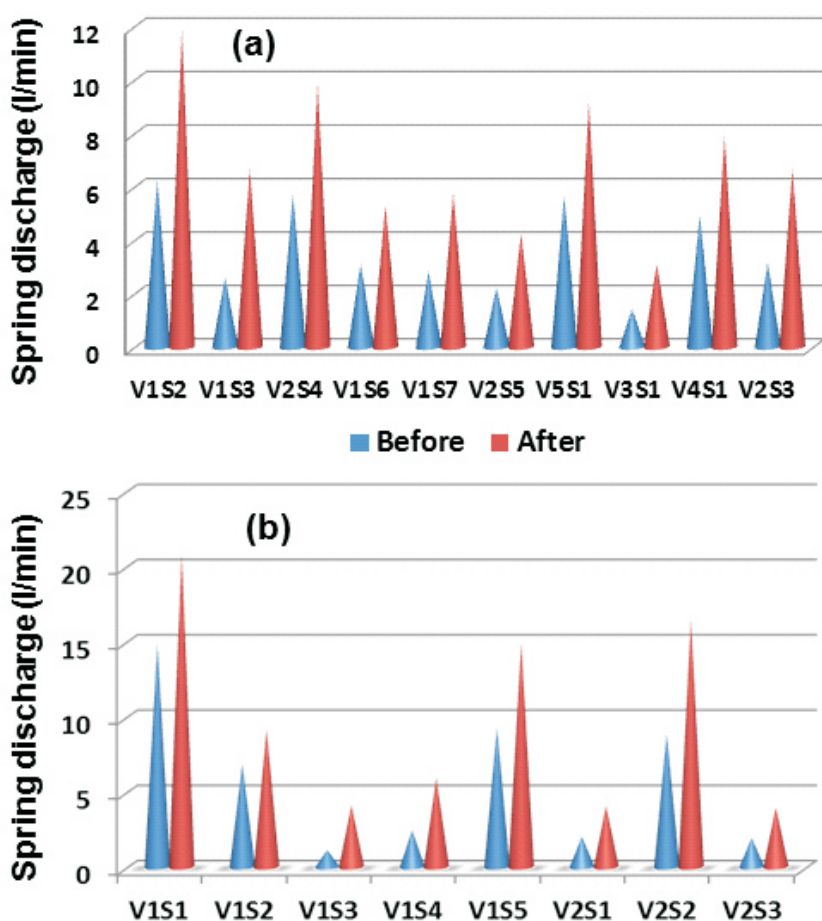


Fig.7:Spring discharges (annual average) before and after the construction of recharge structures, a) Pipaya and b)Brahmakhal sites

artificial recharge structures on the spring discharge, monthly monitoring of spring discharges was undertaken before and after the construction work. The rainfall also was measured at these sites during 2008-2014. It is found that the construction of artificial recharge structures has benefited the local communities significantly. The spring discharges were found to increase in all the sites. The increase in spring discharge at Pipaya site is found to be 60-155% (Fig. 7a) and at Brahmakhal site it is 33-248 % (Fig. 7b).

Summary and Conclusion

Springs are the major available sources of water supply for domestic, agricultural and other uses in mountainous regions. The number and

discharge rates of springs are dwindling at a faster rate causing hardship to the local communities particularly during summer period when the availability of spring water becomes too meager for supporting life. Therefore, these resources must be preserved and protected not only for the benefit of the residents but also for ecology and environment. Environmental isotopes have been very instrumental in understanding the spring water recharge, its linkage with local precipitation, subsurface travel times and impact of anthropogenic activities. In the present study, two sites of Uttarakhand state are investigated using environmental isotope tracers (^2H , ^3H and ^{18}O) to identify the dominant recharge altitude of the

drying springs and suggested various methods to augment the spring recharge by construction of artificial recharge structures.

The isotope content of the springs also found to vary based on their altitude as well as season of sampling. Based on the $\delta^2\text{H}$ versus $\delta^{18}\text{O}$ plot of the spring samples, it can be deduced that spring water is mainly recharged from rainwater. The impact of evaporation effect was higher in Pipaya site compared to Brahmakhal site. The environmental tritium data of the spring water also supports the recharge from modern precipitation. The ^3H data of the spring water is similar to that of rainwater, indicating that the travel times are typically in the order of few months. The altitude effect for each spring site is estimated from the relationship of precipitation isotope data with respect to altitude. The altitude effect is estimated to be -0.26 to -0.31 ‰ for $\delta^{18}\text{O}$ per 100 m rise elevation for different sites. Based on the spring discharge data, altitude effect and local geomorphology, the most dominant recharge zones for each site have been identified. The estimated altitudes of the recharge zones in Pipaya and Brahmakhal sites are in the range of 1350-1500 m and 1200-1760 m amsl respectively. The spring discharges were monitored monthly, before and after the construction of the recharge structures. The spring discharges are found to increase in all the sites. The increase in spring discharge at Pipaya and Brahmakhal sites are in the range of 60-155% and 33-248% respectively.

It is evident from the above study that recharge area/s and sources of springs can be identified using the

environmental isotopes in the mountainous region. The isotope results can be integrated with the available hydrogeology and geomorphology to demarcate the recharge zones of the springs. Accordingly, suitable measures can be taken up to increase the longevity of the springs with increased discharge. Information gathered through isotope approach, along with the other complementary data, will help in comprehensive understanding of the hydrogeologic processes associated with Himalayan springs, and can lead to scientifically validated watershed intervention and monitoring plans.

***Corresponding author**

Dr. Tirumalesh Keesari

Acknowledgement

Authors thank Prof. Anil Joshi, Director, HESCO, Dehradun for his support and guidance. Help extended by Shri S.N. Kamble and Shri Ajay Jaryal of Isotope Hydrology Section, IRAD (BARC) in the sampling and measurement of the isotopes is also acknowledged. We thank the anonymous reviewer for the valuable suggestions.

References

1. Agarwal, A., Bhatnagar, N.K., Nema, R.K., Agrawal, N.K. (2012) Rainfall dependence of springs in the Midwestern Himalayan Hills of Uttarakhand. *Mountain Research and Development* 32(4): 446-455.
2. Alford, D. (1992) Streamflow and sediment transport from mountain watersheds of the Chao Phraya Basin, northern Thailand: A reconnaissance study. *Mountain Research and Development* 12(3): 257-268.
3. Bartarya, S.K. (1991) Watershed management strategies in Central Himalaya: The Gaula River Basin, Kumaun, India. *Land Use Policy* 8(3): 177-184.
4. Bonacci, O. (1993) Karst springs hydrographs as indicators of karst aquifers. *Hydrological Sciences Journal* 38(1): 51-62.
5. Bruijnzeel, L.A.; Bremmer, C.N. (1989). Highland-lowland interactions in the Ganges Brahmaputra River Basin: A review of published literature. ICIMOD Occasional Paper No. 11. Kathmandu, Nepal: International Centre for Integrated Mountain Development (ICIMOD). 152p.
6. Clark, I. and Fritz P. (1997) *Environmental Isotopes in Hydrogeology*, Lewis Publishers.
7. Craig, H. (1961) Isotopic variation in meteoric waters, *Science*, 133, 1702-1703.
8. Gupta, A. and Kulkarni, H. (2018) Report of Working Group I: Inventory and Revival of Springs in the Himalayas for Water Security, NITI Aayog report, pp 1.-54.
9. Jeelani, G. Bhat, N.A., Shivanna, K. (2010) Use of $\delta^{18}\text{O}$ tracer to identify stream and spring origins of a mountainous catchment: A case study from Liddar watershed, western Himalaya, India. *Journal of Hydrology* 393(3): 257-264.
10. Jeelani, G. Kumar, U.S. Bhat, N.A. Sharma, S. Kumar, B. (2015) Variation of $\delta^{18}\text{O}$, δD and ^3H in karst springs of south Kashmir, western Himalayas (India). *Hydrological Processes* 29(4): 522-530.
11. Keesari Tirumalesh, Shivanna, K., Noble, J., Narayan, K. K. and Xavier, K. T. (2007) Nuclear techniques to investigate source, origin of groundwater pollutants and their flow path at the Indian Rare Earths Ltd, Cochin, Kerala. *J. Radioanal. Nucl. Chem.*, 274, 307-313.
12. Kendall, C. and Caldwell, E.A. (1998) Fundamentals of isotope geochemistry. In: *Isotope tracers in catchment hydrology*, eds., Kendall, C.; McDonnell, J.J. Pp. 51-86.
13. Kulkarni, U. P. (1992) Radiotracer experiment to identify the location of seepage areas in the Borda minor irrigation tank, Yeotmal district, Maharashtra. In *Proceedings of the Nuclear and Radiochemistry Symposium*, Visakhapatnam, pp. 311-313.
14. Mahamuni, K.; Kulkarni, H. (2012) Groundwater resources and spring hydrogeology in South Sikkim, with special reference to climate change. In: *Climate change in Sikkim - Patterns, impacts and initiatives*, eds., Arrawatia, M.L.; Tambe, S. Gangtok, India: Information and Public Relations Department, Government of Sikkim. Pp. 261-274.
15. Pant, C.; Rawat, P.K. (2015) Declining changes in spring hydrology of non-glacial river basins in Himalaya: A case study of Dabka Catchment. In: *Dynamics of climate change and water resources of Northwestern Himalaya*, eds., Joshi, R.; Kumar, K.; Palni, L.M.S. Part of the series

- Society of Earth Scientists Series.
Pp. 151-179.
16. Rangarajan, R. and Athavale, R. N. (2000) Annual replenishable groundwater potential of India – An estimate based on injected tritium studies. *J. Hydrol*, 234, 38–53.
 17. Rao, S. M. (1984) Injected radiotracer techniques in hydrology. *Proc. Indian Acad. Sci. (Earth Planet. Sci.)*, 99, 319–335.
 18. Shivanna, K.; Tirumalesh, K.; Noble, J.; Joseph, T.B.; Singh, G.; Joshi, A.P.; Khati, V.S. (2008) Isotope techniques to identify recharge areas of springs for rainwater harvesting in the mountainous region of Gaucher area, Chamoli District, Uttarakhand. *Current Science* 94(8): 1003-1011.
 19. Tambe, S.; Kharel, G.; Arrawatia, M.L.; Kulkarni, H.; Mahamuni, K.; Ganeriwala, A.K. 2012. Reviving dying springs: Climate change adaptation experiments from the Sikkim Himalaya. *Mountain Research and Development* 32(1): 62-72.
 20. Valdiya, K.S.; Bartarya, S.K. (1989) Diminishing discharges of mountain springs in a part of Kumaun Himalaya. *Current Science* 58(8): 417-426.
 21. Vashisht, A.K. (2008) Ingenious techniques for irrigation sustainability in Himalayan and Shiwalik foothill regions. *Current Science* 95(12): 1688-1693

Advanced Mirror Alignment System for Indus-2 DEXAFS Beamline

Sumit Kumar Sinha*, Abhishek Jaju, T. A. Dwarakanath,
Gaurav Bhutani, K. Madhusoodanan

Division of Remote Handling & Robotics

Debdutta Lahiri, Nandini Garg

High Pressure & Synchrotron Radiation Physics Division

S. N. Jha, Ashutosh Dwivedi

Atomic & Molecular Physics Division

Abstract

Experiments carried out at High Pressure XAFS facility at BL-8 beamline of Raja Ramanna Centre for Advanced Technology (RRCAT) require high precision alignment of focusing optics (mirror) for targeted focusing of X-ray beam at the sample. A high-precision six Degree of Freedom (DoF) system characterized by a very fine resolution ($1\mu\text{m}$ in translational and 1 arc-second in rotation) was designed and successfully installed at BL-8 to this effect. As part of this exercise, an X-X' telescopic platform has also been designed and successfully deployed to align the mirror chamber along the beamline traversing from the Goniometer. Beamline specific fixtures, operational aspects as well as technology demonstration of BL-8 beamline arrangement have been discussed in this paper.

Keywords: Synchrotron beam alignment system, 6 DoF Hexapod mechanism, High pressure XAFS, DEXAFS, HPXAFS, Mirror chamber manipulation

Introduction

DEXAFS (Dispersive Extended X-ray Absorption Fine Structure) beamline (BL-8) at Indus-2 is dedicated to nano-scale structural and chemical understanding of matter with XAFS technique [1]. Optical layout of DEXAFS beamline (BL-8) is shown in Fig. 1, where polychromator (CC) selects a band of energy from the white synchrotron beam, horizontally disperses it and focuses on to the sample (S1). The transmitted beam from the sample is recorded on a position sensitive detector (D), thus enabling recording of the whole XAFS spectrum. Static and focusing optics of DEXAFS configuration is particularly ideal for High Pressure XAFS (HPXAFS) experiments, which is the key to understanding geophysical, mechanical and

electronic transitions of matter under pressure. These Diamond-Anvil-Cell (DAC) based specialized experiments have $< 100\ \mu\text{m}$ sample size and therefore, require further reduction

from the present focal spot size at BL-8. Additional vertically-focusing bendable Rhodium mirror (M1) was designed and installed for this purpose (Fig. 1). X-ray beam is reflected off

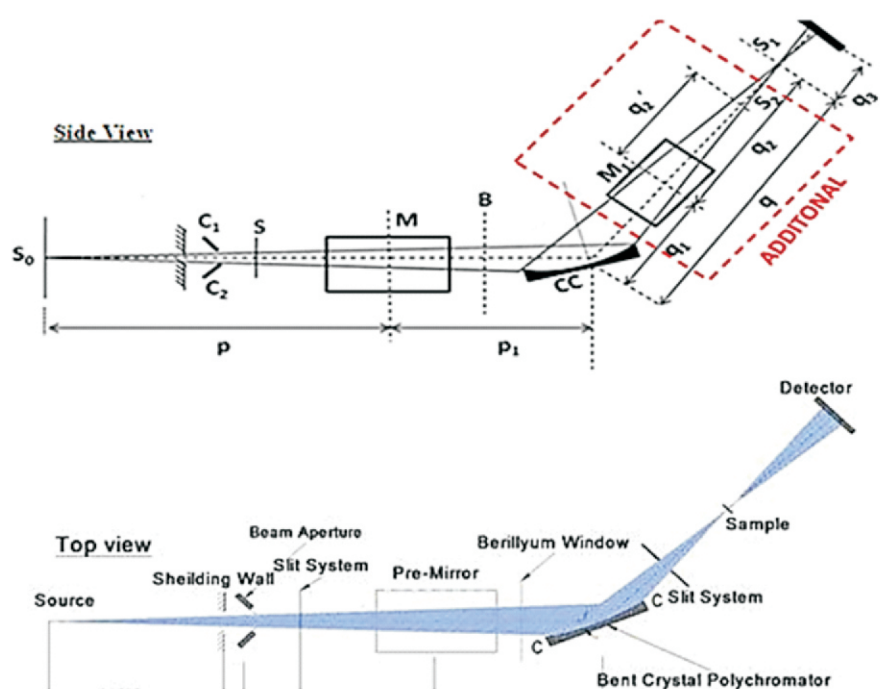


Fig.1. Optical Layout of DEXAFS beamline (BL-8) in RRCAT

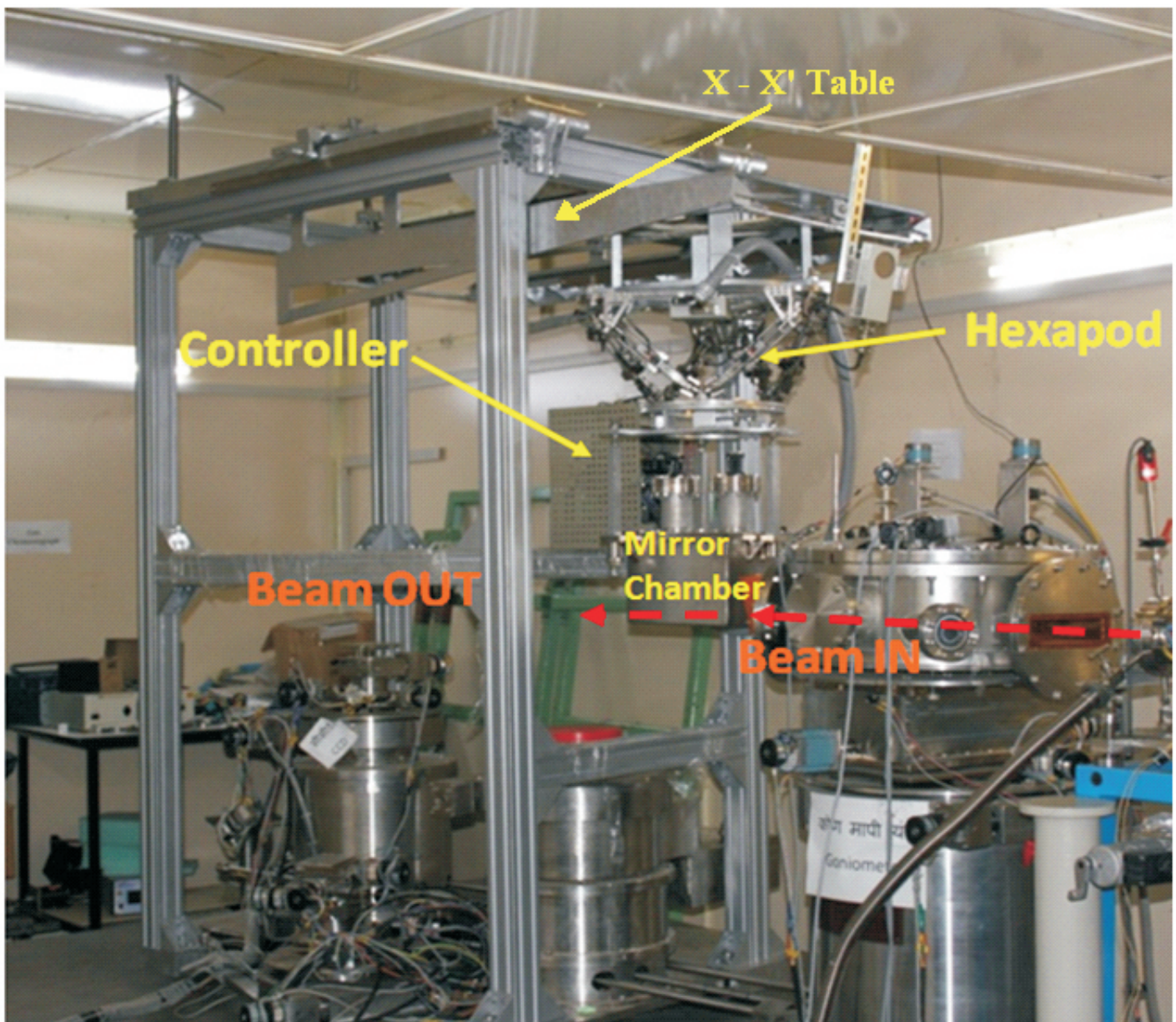


Fig.2. Hexapod based high precision beam alignment system at BL-8, INDUS-2, RRCAT

the mirror (M1) and focused at new position (S2). Good focusing requires precise centering of the mirror (M1) on the beam. In the first phase of HPXAFS commissioning [2], focusing exercise with manual movement of the mirror stage was arduous, highly time consuming and did not lead to the targeted precision of alignment. This has necessitated the development of a multi-axis high precision motorized mirror (M1) stage. In order to meet the objective, Division of Remote Handling & Robotics, Bhabha Atomic Research

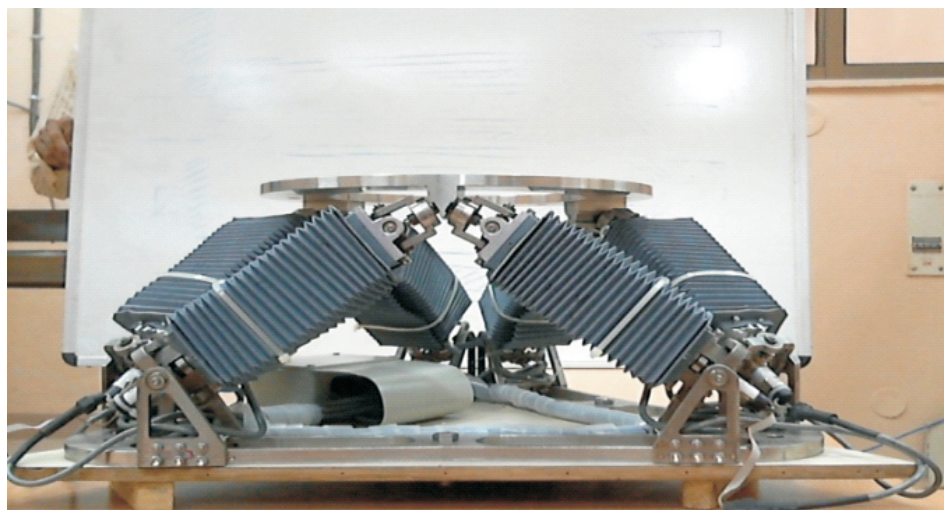
Centre has developed a six DoF hexapod which is suspended on a telescopic X-X' linear table. Further the mirror chamber is rigidly suspended on the hexapod using a set of length adjustable double locking bolts. The mirror located inside the chamber can be manipulated both in position and orientation in all the directions.

The arrangement is shown in Fig. 2. The mirror can be steered to make the focused beam to reflect on the target. Its salient features include:

- The X-X' table has 2 DOF telescopic motions along the beamline.
- X-X' table structure has additional 2 DOF - one translational along the beam direction and one rotational about central axis of the Goniometer.
- The hexapod system provides high resolution alignment of the mirror with the beamline.
- Ease of mounting and dismounting of mirror chamber is feasible.

Table 1: General Specifications

Total Degree of Freedom (DOF) of the system	8
Payload	80 kg
Maximum X movement	1.5 m
Hexapod Degree of Freedom (DOF)	6
Translational Resolution in along all Directions	1 μm
Rotational Resolution about all Directions	1 arc-second

**Fig.3. Lock of X' axis of X-X'Table****Fig.4. Parallel Mechanism based Hexapod System****Methodology for Alignment**

Bendable Rhodium mirror (M1) is mounted inside a sealed chamber having transparent windows of size 28mm \times 28mm for X-ray beam inlet & outlet. The X-ray beam is reflected off the mirror within the chamber. The

X axis of the X-X'table is motorized and can be operated directly through the computer interface. The X' axis of the X-X'table is manually operated for the initial adjustment of the mirror chamber and can be locked with its locking arrangement at any location

(Fig.3). The hexapod is used to provide controlled motion for highly precise alignment both in position and orientation about the mirror axes. The hexapod is a 6 DoF (three translational & 3 rotational) parallel mechanism based mechanical system with six legs (Fig.4). The advantage of hexapod is its high payload capacity and high positional accuracy. The basic principle is that for achieving any position and orientation of the platform, a unique joint space comprising of six leg lengths can be determined. The leg lengths can be controlled in a coordinated fashion to achieve predetermined leg lengths. The fine tuning to focus the beam on sample can be done with the help of the hexapod system with very fine resolution of 1 μm in translations and 1 arc-second in rotations independently about all three perpendicular directions.

The X-X'table is designed in such a way that the whole setup can be moved sideways from the beamline and the mirror chamber can be removed easily from the path of beamline to facilitate other experiments. The alignment system is controlled by a computer interface (Fig.5). Software for kinematics, control and user interface was developed in-house. The software provides user interface to manipulate X-axis of X-X'table motion as well as 6 axes hexapod to align the mirror so as to control the beam reflection. Historical position of mirror can be stored and can be reused to orient the mirror subsequently.

Testing and Calibration

To evaluate the performance of the hexapod system, repeatability and accuracy checks at various payloads

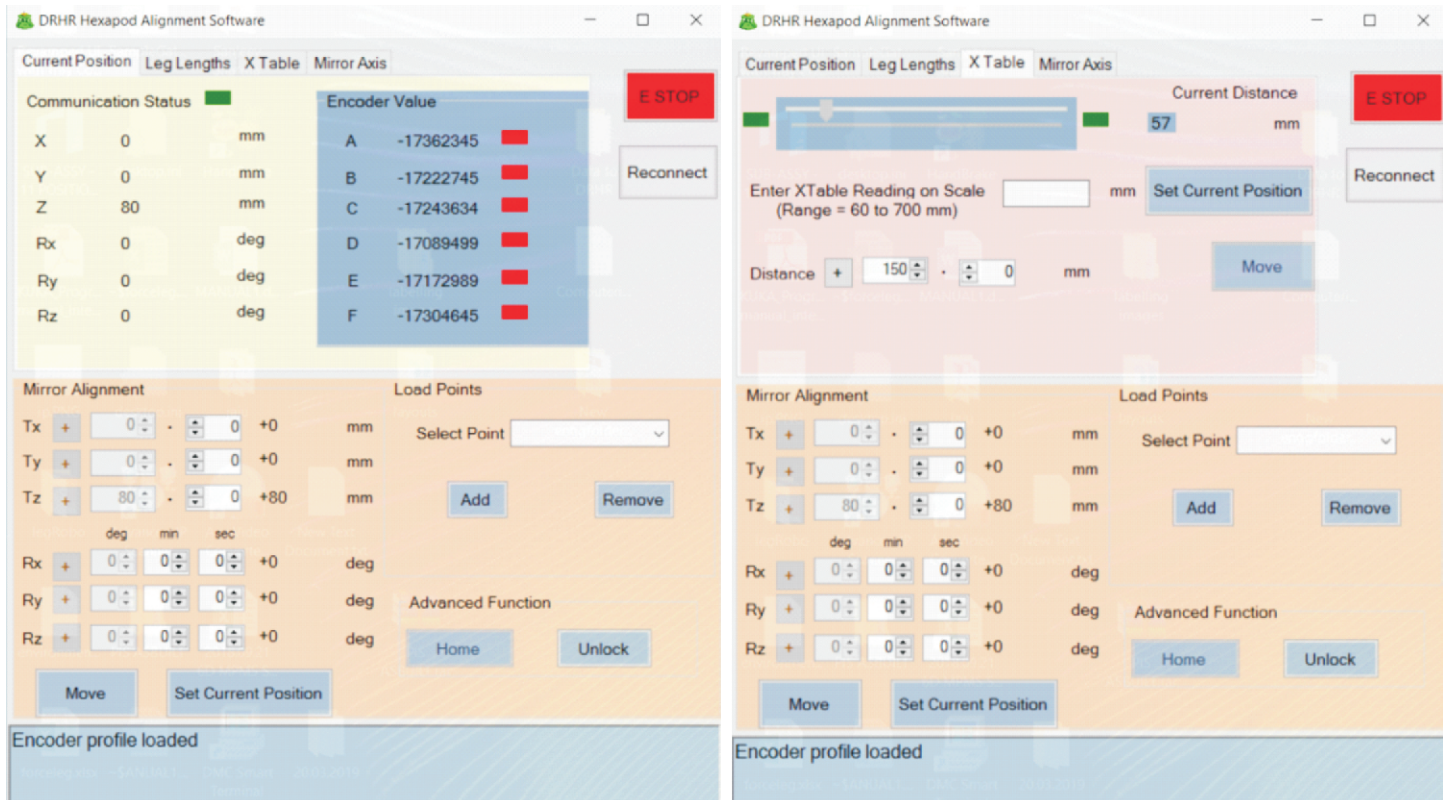


Fig.5. Computer interface for beam alignment system



Fig.6. Load Testing and Calibration

were carried out. The repeatability of hexapod unit in achieving a position along three mutually perpendicular axes was measured individually using standard Coordinate Measuring Machine (CMM) in a metrological laboratory (Fig.6). The hexapod unit is fed with an input along each axis to achieve a pre-defined position several times. The repeatability of the unit to reach the given position was evaluated. Repeatability of position along a specific direction is found to be within $5\ \mu\text{m}$. The deviation if any to reach a given position from all the directions was also evaluated. The repeatability of the hexapod [3] unit is within $14\ \mu\text{m}$. The accuracy check of the hexapod unit was carried out by measuring the actual position and orientation of the platform with respect to rigid base frame for a given theoretical position and orientation of the platform. The platform of hexapod unit was commanded to move at

various positions using motion controller. Position sensors at the joint space were used to determine the actual position and orientation. The volumetric error of the hexapod unit is within $67\mu\text{m}$.

Results

The system adheres to all the general specifications listed in table 1. Beamline alignment by manipulating the mirror with very fine resolution: $1\mu\text{m}$ in translations and 1 arc-second in rotations are feasible. Independent motion about all three perpendicular directions and/or controlled coordinated motion along arbitrary direction are feasible. The repeatability and accuracy of the hexapod system are within $14\mu\text{m}$ and $67\mu\text{m}$ respectively. The system has been tested for beam alignment using the control interface. Alignment was demonstrated very precisely and the

position was stored for future reorientation. CCD detector showed the reflected beam. Also the X-X' table motions were demonstrated. A hexapod with equivalent operating characteristics developed by Division of Remote Handling and Robotic, BARC for regulating the mirror assembly for ARPES at BL-10 is providing stable and accurate posturing requirements since 2016.

Conclusion

The six DoF hexapod system along with X-X' table has been developed for very high precision application. Specific beamline constraints are considered. The capability of design, development and deployment is demonstrated.

***Corresponding author**

Shri Sumit Kumar Sinha

References

1. RRCAT Indore, India, <http://www.rrcat.gov.in/technology/accel/srul/beamlines/exafs.html> (Last Accessed, January 16, 2020).
2. N. Ramanan et al., "First phase commissioning of high pressure XAFS setup at ED-XAFS beamline, Indus-2 synchrotron radiation source, India", *J. Opt.*, 44(2), (2015):182–194.
3. Sumit Kumar Sinha, T. A. Dwarakanath, Abhishek Jaju, "Six DOF Mirror Alignment System for Beam line Applications", Presented in 3rd International and 18th National Conference on Machines and Mechanisms (iNaCoMM 2017), held by Bhabha Atomic Research Centre, Mumbai, from 13th Dec. to 15th Dec. 2017.

Back Page Photo: Homi Jehangir Bhabha and DAE staff are seen together with the personnel of UK nuclear energy establishment at the CIR construction site in Trombay c. 1957-59.
(DAE Archives)



Edited & Published by:
Scientific Information Resource Division
Bhabha Atomic Research Centre, Trombay, Mumbai 400 085, India
BARC Newsletter is also available at URL:<http://www.barc.gov.in>